THE ASTROPHYSICAL JOURNAL, 435:L63–L66, 1994 November 1

STELLAR PHOTOMETRY INCLUDING SATURATED IMAGES: RESULTS ON M67 WITH WFPC2[1]

RONALD L. GILLILAND[2]
Received 1994 May 16; accepted 1994 August 15

ABSTRACT

The Wide Field and Planetary Camera 2 (WFPC2) on *HST* is providing unsurpassed imaging capabilities and supporting accurate stellar photometry over large fields of view at high angular resolution. I discuss a feature of the WFPC2 CCD systems that nominally limits the dynamic range attainable with single exposures: a 12 bit analog to digital converter that does not allow sampling of the CCD full-well depth even at the low gain ($14e^-$/DN) setting. I demonstrate that accurate stellar photometry can be performed on stellar images that are strongly saturated. Two 40 s exposures in *V* and *I* bands on the old open cluster M67 are analyzed to demonstrate photometric capabilities with a dynamic range of over 12 mag from single exposures. New photometric results for both bright and faint objects in M67 are derived from the WFPC2 data.

Subject headings: binaries: visual — methods: data analysis — open clusters and associations: individual (M67) — techniques: photometric

1. INTRODUCTION

As will be amply demonstrated by the ensemble of *Letters* in this issue, the Wide Field and Planetary Camera 2 (WFPC2) provides *HST* with the originally intended high angular resolution imaging capabilities over wide fields of view. It is not the purpose of this paper to provide a comprehensive discussion of photometry with WFPC2; rather I explore in some detail a feature that influences attainable dynamic range at the bright limit in WFPC2 data. I describe a technique allowing accurate (to ~2%) photometry on stellar images that are up to 6 mag brighter than the saturation limit. Since observing time on *HST* is highly oversubscribed, there will often be a reluctance to take multiple exposures at widely spaced integration times to allow proper sampling of both bright and faint targets that are often within a field.

M67 is a rich open cluster of roughly solar age and metallicity that has been among the best-studied targets photometrically, both in the era of photoelectric detectors (Eggen & Sandage 1964) and with CCDs (Montgomery, Marschall, & Janes 1993, hereafter MMJ). For typical ground-based observations, M67 provides as crowded a field (typical separations of ~10″) as can be observed to high photometric precision without having to resort to analysis of blended images. For *HST* observations, M67 provides a sparse field containing just enough stars per CCD to support a photometric analysis.

Single 40 s exposures near the center of M67 in *V* (F555W) and *I* (F814W) were taken on 1994 January 21 as part of the *HST* Servicing Mission–Orbital Verification (SMOV) program for WFPC2 photometric calibration (John Trauger, principal investigator). These images (rootnames u22u0501t and u22u0502t) are part of the publicly available data archive. The F814W image of M67 is shown in Figure 1 (Plate L29). The WFPC2 field on M67 contains 25 stars of 10th to 18th magnitude with well-determined ground-based *V* and *I* photometry (MMJ; Gilliland et al. 1991), but only seven of these are unsaturated in both exposures (PC1 and WF4 have only one unsaturated calibration star each). An additional seven objects fainter than 18th magnitude are readily visible in both of the WFPC2 data frames, but we lack reliable published photometry for comparison. Clearly, to make full use of these M67 observations as a test of WFPC2 photometric capabilities, we require photometric calibration of saturated images. Placing normal and saturated images on the same intensity scale requires knowledge of how many electrons are in a fully saturated pixel, and an algorithm for counting the number of saturated pixels [in units of intrinsic full-well depth, not just the readily apparent analog to digital converter (ADC) limit].

An ideal empirical basis for calibration of the CCD well depths would consist of two images taken at both a short exposure time with well exposed, but unsaturated profiles, and a long exposure in which the same stars are well saturated. The full-well depth per pixel can then be derived simply as the multiplicative term required to maintain a linear scaling of total counts at the known exposure time ratio. A search of the *HST* data archive for *V* and *I* exposures through 1994 March 7 turned up two programs with proprietary data that with the observer's permission was analyzed in order to calibrate full-well depths. The ERO observations of R136 (J. Trauger, principal investigator, program 5590) were obtained 1994 January 2 at exposure time ratios of 20 in F814W, and 10 and 50 in F555W. GO observations (S. Strom, principal investigator, program 5355) obtained in 1994 February provided F814W images with exposure time ratios of 100. All of the exposures were doubled (for cosmic-ray elimination) at both the short and long exposure times, thus allowing for independent full-well depth determinations over two data pairs. Thirty images in total were analyzed containing 146 pairs of stars allowing full-well depth determination. All of the data were analyzed after standard pipeline data reductions (Burrows 1994). The M67 data were run through standard STSDAS reductions to take advantage of improved flat fields.

2. CALIBRATION OF CCD FULL-WELL DEPTHS

In this *Letter* I rely on simple aperture photometry and saturated pixel counting for stellar image intensity extractions. The WFPC2 CCDs have full-well depths of order $90{,}000e^-$

[1] Based on observations with the NASA/ESA *Hubble Space Telescope* obtained at the Space Telescope Science Institute, which is operated by Association of Universities for Research in Astronomy, Incorporated, under NASA contract NAS5-26555.

[2] Space Telescope Science Institute, 3700 San Martin Drive, Baltimore, MD 21218.

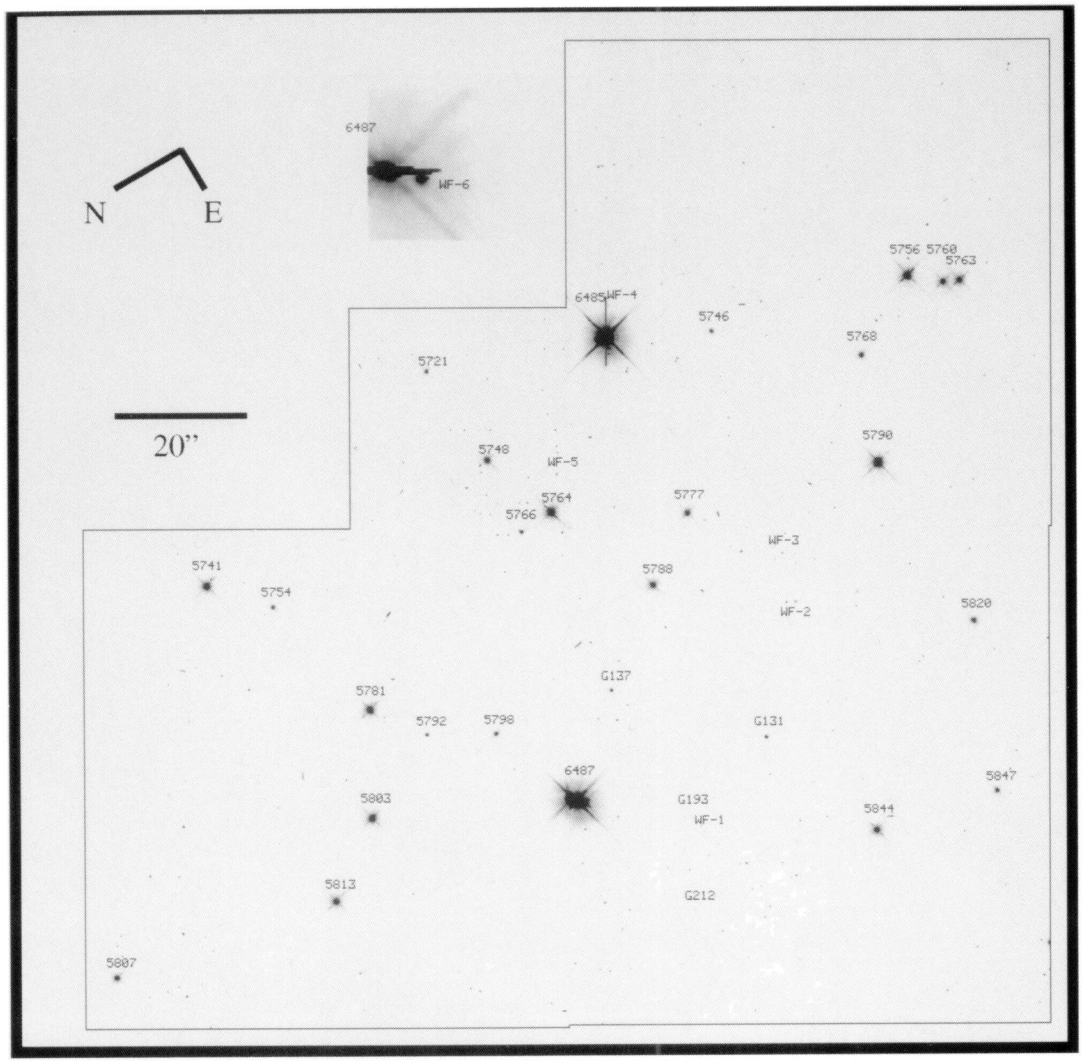

FIG. 1.—Four CCD mosaic of M67 in F814W (40 s exposure) with WFPC2. Star IDs with numerical values are from MMJ, IDs starting with G are from Gilliland et al. (1991), and WF-x objects are new detections (see Table 3 for photometry). The insert image shows a ×4 magnified view of the 10th magnitude object No. 6487 showing that this is at least an optical double and may be a triple.

(Burrows 1994). The 12 bit ADC imposes a limit of 4095 DN, with ~300 DN being used as a bias offset the gains of 7 and 14e^- sample 26,500 and 53,000e^- (~30% and ~60% of physical full-well depth), respectively. Any pixel with a value of 4095 in the *raw data* had an intensity level that equaled or exceeded the ADC limit and therefore only bounds exist on how many e^- should be counted for the pixel. For a pixel in the middle of an extended bleeding column it is valid to assume the pixel reached full-well depth and then began passing additional charge through. For an image that contains only one (ADC) saturated pixel in the core the saturated pixel count, N_s, will be $0.3 \leq N_s \leq 1.0$, this for gain of 7e^-/DN, at 14e^-/DN the lower limit is ~0.6.

Given the same star observed for a short time, t_1, that does not lead to even ADC saturation, and a much longer exposure, t_2, with many resulting saturated pixels, N_s, the following equation may be solved for the physical full-well depth, FW:

$$\text{counts}_1/t_1 = (\text{counts}_2 + \text{FW} \times N_s)/t_2 , \quad (1)$$

where counts is the number of events in electrons (DN × gain). The counts are simply sums over all non-ADC saturated pixels in a specified aperture using the pipeline calibrated data. The fraction of FW sampled by the data values is

$$\text{FS} = (4095 - \text{bias})q/\text{FW} , \quad (2)$$

where the bias level (DN) depends on gain ($q \equiv e^-$/DN) selected and the particular CCD; Table 1 gives current values for bias and gain levels (Burrows 1994). Also included in Table 1 are the full-well depths (FW) in e^- and the slope of FW with number of saturated pixels in a single image (FWS with units of e^-/N_s), the derivation of which will be explained below. The value of FS ranges from 0.29 for WF2 at $q = 7$ to 0.69 for PC1 operated at $q = 14$.

An algorithm to estimate what remaining fraction of FW is filled for a given ADC saturated pixel should depend on analysis only of its two nearest neighbors along the columns—this assures a simple and robust technique for counting saturated pixels along the primary charge trails. Unsaturated images may be analyzed to calibrate an algorithm to estimate the intensity level in a central pixel based on the measured intensity of nearest column neighbors:

$$N_s = \sum_{i,j} \min [1.0, \text{FS} + \max (0.0, d_{i,j-1} + d_{i,j+1} - 2 \times \text{bias} - A)/D] , \quad (3)$$

where the sum over i, j extends over specified apertures and continues along any bleeding trails outside the standard aperture, the $d_{i,j\pm1}$ are values in the raw data which by definition take the value 4095 at ADC saturation. The number of saturated pixels is first developed from the raw data, but must be corrected for any flat-field deviations (multiply local inverse flat onto N_s). The parameter A provides the (bias-subtracted) zero point offset beyond which $d_{i,j}$ is expected to show ADC saturation. The parameter D determines how quickly the residual FW of the pixel at i, j is filled up as a function of increasing adjacent pixel values. Defining the ratio of adjacent values (depends on subpixel centering),

$$R = \min (d_{i,j-1}, d_{i,j+1})/\max (d_{i,j-1}, d_{i,j+1}) , \quad (4)$$

it is easy to justify selection of

$$A = \max (B, 5400 + R \times C) , \quad (5)$$

$$D = \min (B/\text{FS} - B, 8190 - 2 \times \text{bias} - B)/(1.0 - \text{FS}) \quad (6)$$

to represent fractional levels of pixel saturation. Table 2 contains the dependence of these parameters on detector and observation wavelength.

With an algorithm for "counting" saturated pixels now in hand it is a simple matter to solve for full-well depths of the CCDs using data appropriate to equation (1). The data sets discussed in § 1 were analyzed as outlined, yielding 30–40 independent determinations of FW for each of the WFPC2 CCDs. Figure 2 shows the derived FW for each CCD plotted against the number of saturated pixels. If charge were perfectly conserved the derived FW would be independent of N_s. Instead, each CCD shows a mild positive trend of FW with N_s, which suggests that either fewer electrons are created at the highest count rates, or charge is lost proportional to the total created.

TABLE 1

GAIN, BIAS, AND FULL-WELL DEPTH VALUES

CCD	q(7)	q(15)	Bias(7)	Bias(15)	FW	FWS
PC1	7.12	13.99	307	294	79321	98.7
WF2	7.12	14.50	348	317	92092	32.5
WF3	6.90	13.95	305	302	81682	118.0
WF4	7.10	13.95	308	305	89516	50.7

TABLE 2

PIXEL SATURATION ALGORITHM PARAMETERS

CCD	Filter	B	C
PC	F555W	2000	−6100
PC	F814W	3200	−4900
WF	F555W	1500	−17700
WF	F814W	2200	−8700

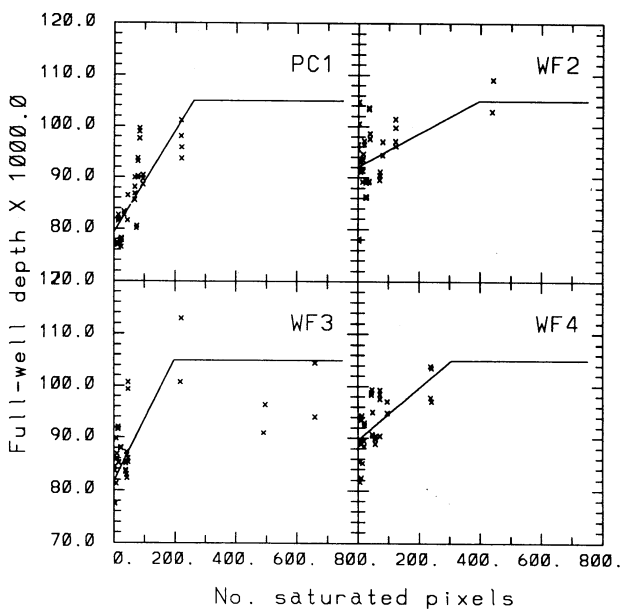

FIG. 2.—Derived full-well depths for each of the CCDs versus number of saturated pixels in a stellar image. Straight line segment from low saturation levels represents a least-squares fit to values with $N_s \leq 450$; an upper limit to FW_e of 105,000e^- is imposed for consistency with the WF3 data.

TABLE 3

NEW M67 PHOTOMETRY

ID	V	$V-I$
WF1.....	22.55	2.31
WF2.....	22.52	2.29
WF3.....	21.32	2.35
WF4.....	21.16	1.41
WF5.....	21.00	2.51
WF6.....	13.47	0.80

In any case, the small effect is easily parameterized to yield an effective full well depth:

$$\mathrm{FW}_e = \mathrm{FW} + N_s \times \mathrm{FWS}\,, \qquad (7)$$

where FW and FWS are given in Table 1 for each CCD. Equation (7) is not well constrained with data for $N_s \geq 250$. A few very strong saturation events for WF3 (see Fig. 2) suggest an upper bound for FW_e of $\sim 105{,}000e^-$ should be adopted, but use of this calibration for N_s greater than 250 pixels (over 6 mag past onset of saturation) is not warranted from this analysis. The scatter of FW about the best-fit lines in Figure 2 is 4%–6% for each CCD. These calibrations utilized data acquired with a gain of $7e^-$ for estimating N_s. Uncertainties at a gain of $14e^-$ should be proportionally smaller since more of the full-well depth is directly sampled.

3. V AND I PHOTOMETRY OF M67

The F555W and F814W frames of M67 provided the motivation for developing an algorithm for counting saturated pixels in order to allow aperture photometry on all of the stellar images present in Figure 1. The M67 data have not been used to provide calibration of the saturated pixel counting algorithm; therefore results from its application to the M67 data serve as an independent test. Intensity extractions have been performed on the M67 data frames using simple digital aperture sums on pipeline calibrated data. Images containing saturated pixels are evaluated as described in the previous section to yield an estimate of N_s. Square apertures of 11 × 11 pixels (WF CCDs) and 23 × 23 pixels (PC1) were used. The number of electrons per second in each image was evaluated from

$$N_e\ \mathrm{s}^{-1} = (\mathrm{counts} \times q + \mathrm{FW}_e \times N_s)/(t_{\mathrm{exp}} \times f_{\mathrm{aper}}) \qquad (8)$$

where counts is the aperture sum in DN of unsaturated pixels, t_{exp} is the exposure time and f_{aper} represents ensquared energy for the above apertures (taken as 0.92 – F555W; 0.94 – F814W).

M67 is well observed from the ground; the most recent photometric study (MMJ) gives both V and I (Cousins) photometry for 25 stars in the WFPC2 field of view. V magnitudes for two fainter stars are taken from Gilliland et al. (1991). Photometric zero points and color terms are solved for to minimize least-squares differences between the published and derived V and I magnitudes. With all of the corrections mentioned below included the solution is

$$V = 24.635 - 2.5 \log_{10} N_e\ \mathrm{s}^{-1}(\mathrm{F555W}) + 0.007(V-I)\,, \qquad (9)$$

$$I = 23.723 - 2.5 \log_{10} N_e\ \mathrm{s}^{-1}(\mathrm{F814W}) + 0.044(V-I)\,, \qquad (10)$$

where V and I are derived magnitudes. The root mean square (rms) deviations with respect to published (27 for V, 25 for I) magnitudes are 0.031(V), 0.025(I) and 0.033($V-I$). The differences (published – calculated) are shown in Figure 3. While these results demonstrate the capability of doing excellent photometry with WFPC2, even on saturated images, the M67 results (eqs. [9] and [10]) should not be adopted as a fundamental photometric calibration; more extensive observations exist for this purpose.

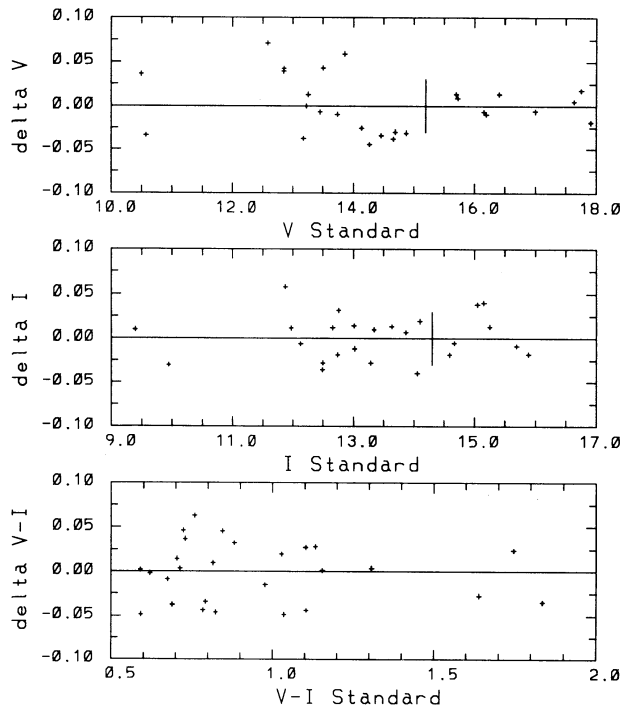

FIG. 3.—Comparison of published and derived photometry in the sense $\delta V = V(\mathrm{standard}) - V$ (as given by eq. [9]); similar for I and $V-I$. Vertical marks in V and I panels show onset of saturation in stellar images for the WFPC2 data.

Several auxiliary corrections have been applied to the aperture intensity results before developing a photometric solution; the first two follow from analyses performed by the WFPC2 IDT (Burrows 1994). In each case the rms discrepancies resulting from dropping these minor corrections are noted in brackets for V and I: (1) The WFPC2 detectors exhibit a minor geometric distortion that influences flat-fields and point source photometry in different ways. To correct for this a normalization term that varies from unity at CCD center to 0.954 at CCD corners as a quadratic function of distance has been multiplied onto the source rate from equation (8) [0.034, 0.025]. (2) A photometric ramp resulting from charge transfer inefficiency results in a count deficit for stars at the top of columns relative to those at the bottom. The effect is present at about the 10% level for faint stars, declining to 5% for brighter (still unsaturated) stars. I found that a (top to bottom in magnitude difference) ramp of 0.08 for stars with $m_V > 15.0$, 0.04 for $14.0 \leq m_V \leq 15.0$ and 0.02 for $m_V < 14.0$ worked well for this solution [0.036, 0.026]. (3) Counts for the PC are multiplied by 1.05; this could result from either aperture size or flat-field normalization differences [0.036, 0.026]. (4) The WF2 and WF3 results for F814W are better if multiplied by 0.97 and 1.03, respectively; again this is suggestive of minor discrepancies with the flat-field normalizations [0.031, 0.033]. These contribute to a qualitatively better solution, but the general discussion of this paper is independent of any or all of these

corrections. The M67 data set analyzed here is not sufficient to address these issues further.

Imaging M67 with 0".1 resolution provides information about close optical multiple stars and faint galaxy/star discrimination that is not available with ground-based imaging even under excellent seeing conditions. Analysis of the two V and I WFPC2 images of M67 has provided new results in both of the above areas. The 40 s F555W and F814W frames support useful photometry to $\sim$22.6(V) and 21.7(I) at which the resulting S/N is $\sim$10.

The insert region of Figure 1 shows detail on a bright star that at WFPC2 resolution is clearly shown to be an optical double and may be a triple. The fainter, but still saturated component labeled WF6 has photometry of $V = 13.47$, $V-I = 0.80$ (errors of about $\pm$0.1 mag apply), values entirely consistent with an upper main-sequence member of M67. The composite image (IDs: 6487, MMJ; 1023, Sanders 1977) has $V = 10.544$, $V-I = 0.627$ (MMJ). Excluding the fainter double, photometry of $V = 10.624$, $V-I = 0.627$ has been adopted for the primary for comparison with WFPC2 based photometry as shown in Figure 3. Perhaps of equal interest is that the diffraction spikes coming off the primary are doubled with a separation of $\sim$0".25, which suggests that the primary is itself a close optical double with nearly equal ($V \sim 11.38$) intensity components. Based purely on proper motions, Girard et al. (1989) derive only a 7% membership probability for this star, including its central position in projection on the cluster raises its membership probability to 45%. Mathieu et al. (1986) cite a radial velocity of 3.6 km s^{-1}, which is well away from the M67 mean of 33.6 $\pm$ 0.7 km s^{-1}. An unresolved system could lead to errors in both the proper motion and radial velocity determinations, thus calling into question the relevance of these published results for testing system membership.

A sharpness statistic, $\Gamma = \sum_i \max(0, P_i)^2/[\sum_i \max(0, P_i)]^2$ (Burrows 1994), has been computed for all unsaturated images, where P_i is the fractional energy of each pixel within a summation over 121 pixels nearest the image center. For eight well exposed stars on the WF CCDs in F814W Γ averages to 0.111 $\pm$ 0.008. The objects G193 and G212 both have $\Gamma < 0.017$ on the F814W exposure and are (by inspection) extended objects at the WFPC2 resolution. These were not detectable as background galaxies in ground-based imaging at 1".5 seeing. The six objects labeled in Figure 1 as WF-x do not have published photometry and all have values of Γ consistent with point sources; photometric results for these newly detected objects are given in Table 3. For these faint objects smaller ($\sim$0".5) apertures were used with corrections applied as determined from brighter stars to place them on the same scale; at $V \sim 21.4$ the photometric error is $\sim$0.06 mag. WF5 has color and magnitude consistent with ($M_V = 11.48$ at $V-I = 2.51$ for the lower main sequence; Stauffer 1982) M67 membership. The stars WF1, WF2, and WF3 are 1–2 mag fainter than indicated for the M67 main sequence and may be background objects.

4. CONCLUDING REMARKS

The physical full-well depth for each WFPC2 CCD has been calibrated. A test with two M67 frames in V and I shows that photometry to an accuracy of $\sim$2% can be maintained for stellar images to at least 5 mag brighter than saturation. Selection of the low ($q = 14e^-$/DN) gain setting supports higher precision on bright objects and imposes generally minor losses at the faint limit. With proper treatment of saturated stellar images photometry over a dynamic range in excess of 12 mag can be performed from single WFPC2 exposures.

I thank S. Baggett, M. Clampin, and J. MacKenty for assistance regarding WFPC2 data reductions. For access to proprietary data in support of full-well depth determinations I am grateful to D. Hunter, S. Strom, and J. Trauger. I have also benefited from discussion and insight provided by C. Burrows, J. Hester, J. Holtzman, A. Saha, and J. Trauger.

REFERENCES

Burrows, C. J., et al. 1994, WFPC2 Instrument Handbook, Version 2.0 (Baltimore: ST ScI)
Eggen, O. J., & Sandage, A. R. 1964, ApJ, 140, 130
Gilliland, R. L., et al. 1991, AJ, 101, 541
Girard, T. M., Grundy, W. M., López, C. E., & van Altena, W. F. 1989, AJ, 98, 227
Mathieu, R. D., Latham, D. W., Griffin, R. F., & Gunn, J. E. 1986, AJ, 92, 1100
Montgomery, K. A., Marschall, L. A., & Janes, K. A. 1993, AJ, 106, 181 (MMJ)
Sanders, W. L. 1977, A&AS, 27, 89
Stauffer, J. 1982, AJ, 87, 899